A Designed Zn^{2+}-Binding Amphiphilic Polypeptide: Energetic Consequences of π-Helicity†

David M. Morgan and David G. Lynn*

Searle Chemistry Laboratory, Department of Chemistry, University of Chicago, Chicago, Illinois 60637, and Departments of Chemistry and Biology, 1515 Pierce Drive, Emory University, Atlanta, Georgia 30322

Hélène Miller-Auer and Stephen C. Meredith*

Department of Pathology, University of Chicago, 5841 South Maryland Avenue, Chicago, Illinois 60637

Received July 2, 2001; Revised Manuscript Received September 5, 2001

ABSTRACT: The π-helix is a secondary structure with 4.4 amino acids per helical turn. Although it was proposed in 1952, no experimental support for its existence was obtained until the mid-1980s. While short peptides are unlikely to assume a marginally stable secondary structure spontaneously, they might do so in the presence of appropriate structural constraints. In this paper, we describe a peptide that is designed to assume a π-helical conformation when stabilized by cetyltrimethylammonium bromide (CTAB) micelles and Zn^{2+}. In the designed peptide, lipophilic amino acids are placed such that it would be amphiphilic in the π-helical, but not in the α-helical, conformation. Also, two His residues are incorporated with i, $i + 5$ spacing, designed to allow binding of Zn^{2+} in a π-helical but not an α-helical conformation. The peptide was found to form moderately stable monolayers at the air−water interface, with a collapse pressure that almost doubled when there was Zn^{2+} in the subphase. Also, CTAB micelles induced a marked increase in the helicity of the peptide. In 50% TFE, the peptide had a CD spectrum consistent with an α-helical structure. The addition of 1 mM Zn^{2+} to this solvent caused a saturable decline in ellipticity to approximately half of its original value. The peptide also bound Zn^{2+} when it was bound to CTAB micelles, with Zn^{2+} again inducing a decrease in ellipticity. The peptide had slightly greater affinity for Zn^{2+} in the presence of the CTAB than in a 50% TFE solution ($K_d = 3.1 \times 10^{-4}$ M in CTAB and 2.3×10^{-4} M in TFE). van't Hoff analysis indicated that thermal denaturation of the peptide in 50% TFE containing 1 mM Zn^{2+} was associated with both enthalpic and entropic changes that were greater than those in the absence of Zn^{2+}. These observations are all consistent with the proposal that the peptide assumed a π-helical conformation in the presence of Zn^{2+} and CTAB micelles, and has allowed the stability of this rare conformation to be assessed.

The concept of secondary structure preceded the development of methods for protein structure determination. Thus, in 1951, Pauling proposed the α-helix as a likely secondary structure (*1*) and the β-sheet as a structure of silk fibroin (*2*). Other secondary structures were proposed at the same time, but these have been observed uncommonly or not at all. One such structure, the π-helix, was proposed by Low and Baybutt in 1952 (*3*). Like the α-helix, the π-helix was proposed to be stabilized by hydrogen bonds, but instead of hydrogen bonds occurring between residues i and $i + 4$ and yielding a helical repeat unit of 3.6 amino acids/turn as they do in an α-helix, in a π-helix, they occur between residues i and $i + 5$ and yield a helical repeat of 4.4 amino acids per turn.

As protein structures were determined, it was observed that α-helices were extremely common, but that π-helices either were extremely rare or did not exist. These observations, as well as theoretical considerations, led to the idea that the π-helix was inherently unstable, but the factors that could account for its instability are unclear. Among the factors that have been suggested to destabilize π-helices are the following. First, the packing of atoms into the interior of the π-helix leaves a central cavity (*3*). No such cavity exists in the α-helix; maintaining such a cavity in a π-helix would result in the loss of van der Waals contacts. Second, steric hindrance increases in a π-helix, as shown in Ramachandran plots, which place the π-helix in a marginally stable region of conformational space (*4*). Third, although the hydrogen bond distances between amide protons and carbonyl oxygens are slightly shorter in the π-helix than in the α-helix, the hydrogen bond dipoles are angled with respect to one another, rather than collinear, as they tend to be in the α-helix (*3*, *5*). Finally, the organization of a single turn of the π-helix involves 16 peptide backbone atoms, compared to only 13 for the α-helix (*3*), resulting in a relatively larger entropic cost for nucleating and maintaining the π-helix.

† This work was supported by NIH Grant (NHLBI) HL 15062 (S.C.M.), NIH Cardiovascular Pathophysiology and Biochemistry Training Grant HL 07237 (D.M.M.), and NIH Grants GM 47369 and RR 12723 (D.G.L.).

* To whom correspondence should be addressed.

10.1021/bi0155605 CCC: $20.00
Published on Web 10/24/2001

The magnitude of these energetic costs is not certain, however, and estimates have ranged from trivial to prohibitive. For approximately the first 30 years of protein structure determination, no π-helices were identified in the protein crystal structure literature. In the past 15 years, however, well-characterized π-helical turns have been identified in catalase (*6*), fumarase (*7*), P450 cytochrome (*8*), and soybean lipoxygenase (*9*, *10*). In soybean lipoxygenase, there are, in fact, two π-helices, one of which is continuous over 14 consecutive residues. Additionally, π-helices have been observed in molecular dynamics simulations (*11*−*13*).

Thus, π-helices do exist and, indeed, may be much more common than had previously been assumed. In a 1996 survey of the Protein Data Bank for i, $i + 5$ hydrogen bonding in helices, Ramakumar found π-helical turns to occur, on average, once in every protein, including left-handed and right-handed variants (*14*). If they are relatively unstable, then π-helices are likely to occur only in special circumstances in which they can be stabilized by other groups within the protein, or by other molecules in their environment, or because they serve some evolutionarily selected function (*15*). This suggestion may help explain why in Ramakumar's survey, π-helices were observed mainly at the ends of α-helices, leading to his speculation that they serve as helix termination signals.

Kaiser and Kézdy proposed that amphiphilic π-helices might be stabilized by an interfacial environment (e.g., lipid−water or air−water interface) (*16*). The π-helix of soybean lipoxygenase appears to be stabilized by the binding of an Fe^{2+} ion by histidine residues with this spacing (*10*). In this paper, we exploit both of these features and describe the design, synthesis, and characterization of a π-helix peptide. Characterization of this peptide demonstrates that i, $i + 5$ interactions are suitably stable to be prepared in a short polypeptide, and will be used to make an experimental measure of the difference in stability between α- and π-helical turns.

MATERIALS AND METHODS

Peptide Synthesis and Purification. Peptides were synthesized on an FMOC-amide resin (Perkin-Elmer, Applied Biosystems) in a quantity of 0.25 mmol using standard FMOC peptide synthesis protocols with an Applied Biosystems ABI 431 peptide synthesizer. Peptide was cleaved from resin using 0.75 g of phenol, 0.25 mL of ethanedithiol, 0.5 mL of thioanisole, 0.5 mL of water, and 10 mL of TFA[1] for 1.5 h at room temperature. Peptide was precipitated from the above mixture using an excess of ice-cold diethyl ether. Peptide was repeatedly washed with ice-cold ether, dried under nitrogen, and then dissolved in a 0.1% TFA/water mixture for purification by reverse phase HPLC using a preparative Zorbax C-18 column. Peptide eluted at approximately 33% acetonitrile from a 60 min gradient from 0 to 60% acetonitrile, all containing 0.1% TFA. The peptide eluted from the column as one main peak comprising >95% of the total absorbance. The identity of the peptide was confirmed by electrospray mass spectrometry. Lyophilized peptide was stored at −20 °C. Peptide was dissolved in pure water at high concentrations immediately before use, and stock solutions were prepared from dilutions of this preparation. Peptide concentrations were determined by measuring the absorbance of the first solution at 280 nm, using a Hitachi spectrophotometer and an ϵ of 5600 M^{-1} cm^{-1} for the tryptophan residue.

Circular Dichroism. Circular dichroic spectra were measured using a JASCO J715 spectropolarimeter containing 1 or 0.1 mm path length cells. Spectra were collected between 250 and 200 nm, with a step size of 0.2 nm, and at a speed of 20 nm/s. Three spectra were recorded and averaged automatically by the instrument. Due to the presence of CTAB micelles, the response time was set to 2 s to smooth the data, and a large bandwidth, 10 nm, was used. The temperature was maintained at 25 °C for 5 min before the spectrum was recorded. All data for the binding curves were recorded in single-wavelength mode, signal averaging at 222 nm for 1 min.

Zn^{2+} Binding in 50% Trifluoroethanol. Binding of peptide in 50% (v/v) TFE to Zn^{2+} was assessed by CD spectroscopy as described in the Results. For these measurements, mixtures of two solutions in 50% TFE (v/v) were made, one containing 1 mM peptide, 1 mM HEPES (pH 6.0), and 100 mM NaCl and the other containing, in addition, 1 mM $ZnCl_2$. The solution containing only 50% TFE (v/v) buffer and NaCl will be termed 50% TFE.

Cetyltrimethylammonium Bromide Binding. CD spectra of peptide were measured at CTAB concentrations above and below the critical micelle concentration. The CMC of CTAB was determined, according to the method of Chattopadhyay (*17*), to be 32.7 μM under the buffer and salt conditions used for samples described herein [100 mM NaCl and 1 mM HEPES (pH 6.0)]. Binding of peptide to CTAB in the absence of Zn^{2+} was assessed using the following procedure. One stock solution was made containing 0.1 mM peptide, 2 mM CTAB, 100 mM NaCl, and 1 mM HEPES (pH 6.0). This solution was diluted with various volumes of another stock solution, identical except that it contained no peptide. Mixtures of these solutions yielded a range of peptide concentrations. To assess the effect of added Zn^{2+}, the same procedure was used except that each solution also contained 0.1 mM $ZnCl_2$ (Aldrich). To assess the binding of Zn^{2+} to the peptide−CTAB complex, the stock solutions were 0.1 mM peptide, 2 mM CTAB, 100 mM NaCl, and 1 mM HEPES (pH 6.0), and another of the same composition but also containing 1 mM $ZnCl_2$. Each binding experiment was performed twice, with identical but independently prepared stock solutions and mixtures of them, to assess error. Binding curves report the mean data of the replications.

Thermal Denaturation. Thermal denaturation experiments were performed using a sample cell regulated by a Pelletier controller in the spectropolarimeter. Data were collected between 5 and 95 °C in 5 °C intervals. After the temperature had been within 0.5 °C of the desired temperature for a continuous period of 30 s, an additional 5 min period of thermal equilibration was allowed. The CD cell was filled almost completely with the solution that was being analyzed, and sealed with a Teflon plug to prevent changes in concentration due to evaporation during the experiment.

[1] Abbreviations: CD, circular dichroism; CTAB, cetyltrimethylammonium bromide; CMC, critical micelle concentration; TFE, trifluoroethanol; FMOC, 9-fluorenylmethoxycarbonyl; TFA, trifluoroacetic acid; HEPES, hydroxyethylpiperazineethanesulfonate; ApoE, apolipoprotein E.

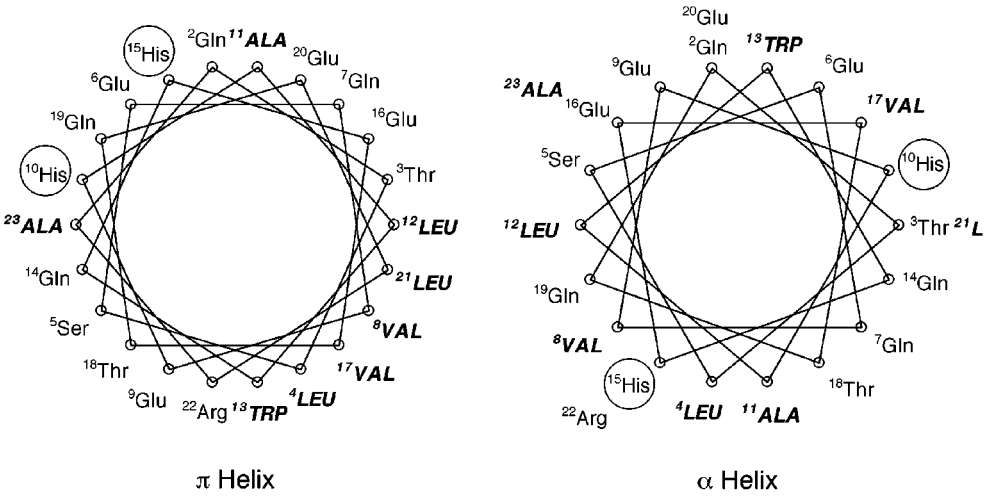

FIGURE 1: π- and α-helical wheels of the designed amphiphilic Zn^{2+}-binding peptide. Hydrophobic amino acids are emphasized (bold, capital, and italic); His residues are circled to show potential Zn^{2+} binding sites. In the π-helical conformation, the hydrophobic amino acids would be aligned on one face of the helical cylinder, and thus, the peptide is predicted to be amphiphilic in this conformation. In the α-helical conformation, no such organization occurs.

Chart 1

1	2	3	4	5	6	7	8	9	10	11	12	13	14	15	16	17	18	19	20	21	22	23	24
	Q	T	L	S	E	Q	V	Q	E	E	L	L	S	S	Q	V	T	Q	E	L	R	A	
G	Q	T	L	S	E	Q	V	E	H	A	L	W	Q	H	E	V	T	Q	E	L	R	A	G

Surface Isotherms. Surface isotherms (surface pressure−area curves) were measured using a Nima Surface Balance equipped with a Pt Wilhelmy plate. Data were collected and stored using Nima Software. The subphase composition was 1 mM HEPES and 100 mM NaCl (pH 6.0), with 0, 1, or 10 mM $ZnCl_2$.

Curve Fitting. Data were fitted to the equations described in the Results using a nonlinear least-squares method provided by the curve fitting functions in IGOR Pro (Wavemetrics) or Kaleidagraph.

RESULTS

Peptide Design. Amino acids 41−61 of human apolipoprotein E, when modeled as a π-helix, are predicted to form an amphiphilic structure; i.e., all of the lipophilic residues align on one face of the putative π-helix (*18*). Although the crystal structure of a thrombolytic fragment of human apolipoprotein E (*19*) shows this domain to consist of a short α-helix linker between two longer α-helices, this sequence was proposed to form a π-helix when ApoE associates with lipoprotein particles (*20*). To promote the formation of a continuous amphphilic π-helix, the following modifications were made to this sequence, and are shown as parent (top) and daughter (bottom) sequences in Chart 1. The relative placement of the hydrophobic and hydrophilic residues in the parent sequence has been retained such that, as shown in Figure 1, all the hydrophobic residues appear to be clustered on one face of the helical cylinder in the π-helical, but not in the α-helical, conformation. A number of modifications were introduced. First, an *i*, *i* + 5 divalent metal binding motif consisting of histidine residues at positions 10 and 15 was incorporated. Second, the Leu at position 13 was replaced with another lipophilic amino acid, tryptophan, to facilitate concentration determination. Third, the ends of the peptide were "capped" by Gly residues; the N-terminus was acetylated, and the C-terminus was amidated. Fourth, the Glu at position 11 was replaced with Ala to preclude the formation of a competing *i*, *i* + 4 metal binding motif between Glu11 and His15. Fifth, Ser at position 14 was changed to Gln to avoid a possible "end-capping" interaction by Ser which might terminate a C-terminal α-helix, an interaction proposed by Luo et al. (*20*) to occur in a homologous peptide.

The overall charge of the original sequence (i.e., when pH > pK_a of the histidine residues) was preserved by reincorporating the two glutamic acid residues removed by the above modifications into positions 9 and 16, flanking the metal binding motif. Although Zn^{2+} is a potential ligand for the glutamate residues in the peptide, the affinity of glutamic acid side chains (i.e., acetic acid) for Zn^{2+} is weaker than that of the histidine side chains (i.e., imidazole) for the first metal−ligand association, and significantly weaker (≥100-fold) for subsequent coordination events (*21*). Additionally, previous work on related peptides containing *i*, *i* + 5 histidine residues had verified the direct involvement of these residues in Zn^{2+} binding through pH dependence studies (data not shown). Consequently, in this peptide, competition for the Zn^{2+} from residues other than histidine was expected to be minimal.

Zn^{2+} Binding to Peptide in 50% TFE. Figure 2A shows CD spectra of the peptide in 50% TFE, 1 mM HEPES, 100 mM NaCl (pH 6), and variable concentrations of Zn^{2+}. The CD spectrum of the peptide in 50% TFE shows two minima, at 208 and 222 nm, consistent with a helical structure. The introduction of increasing concentrations of Zn^{2+} to the peptide in 50% TFE results in a large, progressive, and saturable decrease in negative ellipticity. The data were

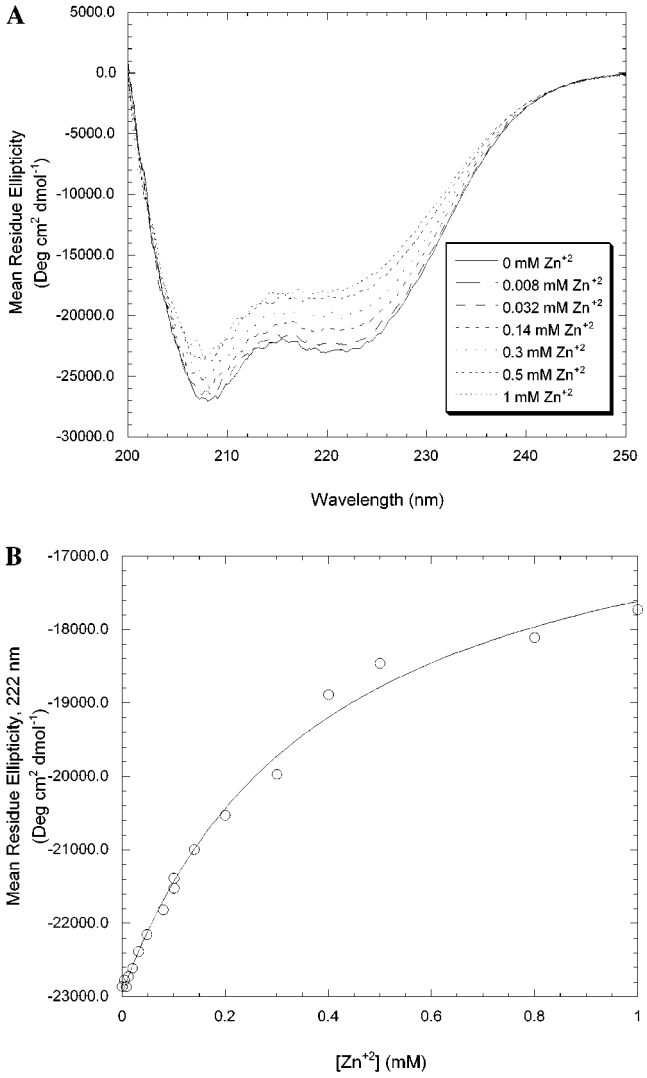

FIGURE 2: (A) CD spectra of the peptide in 50% TFE, at various concentrations of Zn^{2+} ranging from 0 to 1 mM. The buffer is 1 mM peptide, 1 mM HEPES (pH 6.0), and 100 mM NaCl; measurements are taken at 25 °C. The CD spectrum of the peptide in 50% TFE (v/v) exhibits two minima, at 208 and 222 nm, consistent with a helical structure. (B) As the Zn^{2+} concentration increases, there is a significant decline in ellipticity at 222 nm. Data were analyzed as reflecting binding of Zn^{2+} to the peptide. Nonlinear least-squares analysis as described in the text gave a K_d of $(3.1 \pm 0.5) \times 10^{-4}$ M.

analyzed according to the following equilibrium:

$$\text{peptide} + Zn^{2+} \rightleftharpoons \text{complex}$$

$$K_d = \frac{[\text{peptide}][Zn^{2+}]}{[\text{complex}]}$$

The equilibrium constant was calculated by noting that the observed ellipticity was composed of contributions from the free peptide in solution and from the Zn^{2+}−peptide complex:

$$[\theta]_{obs} = f_{complex}[\theta]_{complex} + f_{free}[\theta]_{free}$$

where $f_{complex}$ and f_{free} are the mole fractions of peptide associated with Zn^{2+} or free in solution, respectively, and $[\theta]_{complex}$ and $[\theta]_{free}$ are the corresponding mean residue ellipticities of the peptide, all at 222 nm. Since $f_{complex} + f_{free} = 1$, it follows that

$$f_{complex} = \frac{[\theta]_{obs} - [\theta]_{free}}{[\theta]_{complex} - [\theta]_{free}}$$

$$K_d = \frac{[\text{free}][Zn^{2+}]}{[\text{complex}]} = \frac{([\theta]_{complex} - [\theta]_{obs})[Zn^{2+}]}{[\theta]_{obs} - [\theta]_{free}}$$

Nonlinear least-squares analysis of the data, shown in Figure 2B, yields a K_d of 3.1×10^{-4} M.

The peptide was observed to have a CD spectrum consistent with a random coil conformation in aqueous buffer at pH 7, and that spectrum was not observed to change with Zn^{2+} concentration up to 10 mM (data not shown). This observation suggests that, in aqueous buffer alone, Zn^{2+} ion does not bind, and hence, does not alter the structure of or induce structure in the peptide.

Effect of CTAB on the Peptide. The peptide was designed so that the hydrophobic and hydrophilic side chains would be spatially segregated to separate faces of a π-helical structure. Initial experiments indicated that the addition of egg lecithin vesicles to the peptide did not induce a change in ellipticity. This was not surprising in view of the negative charge of the peptide and the fact that lecithin vesicles have a negative surface potential. Accordingly, we investigated the effect of the cationic detergent CTAB on the CD spectra of the peptide.

As shown in Figure 3A, the CD spectrum of the peptide (80 μM) in aqueous buffer is consistent with that of a random coil with a low helical content, and this is also true in buffer containing submicellar CTAB (0.025 mM). In fact, these two are essentially superimposable, suggesting that the peptide does not interact with the CTAB monomer. In contrast, and as also shown in Figure 3A, the peptide undergoes a significant increase in helical content in the presence of micellar CTAB (2 mM), suggesting that the peptide interacts with the micellar form of the detergent. However, a priori, it is possible that an increase in helicity at 2 mM CTAB could be due to the availability of additional monomeric CTAB arising through dissociation of micelles when the peptide is added to the solution. To confirm that the peptide does not interact with the CTAB monomer, the concentration dependence of the peptide's ellipticity was assessed in aqueous buffer containing submicellar (0.025 mM) CTAB. These data (Figure 3B) show that even when the CTAB monomer is present in excess of peptide, the mean residue ellipticity of the peptide does not change with peptide concentration and, even at the relatively high CTAB:peptide ratios, does not approach the value attained in the presence of CTAB micelles. Thus, the data in Figure 3A are most consistent with the notion that the peptide binds to micelles per se, and this binding induces helical structure.

CD spectra of the peptide at various concentrations in the presence of 2 mM CTAB were measured, and the results are shown in Figure 3C, where mean residue ellipticity is plotted as a function of peptide concentration. At the higher peptide:CTAB ratios, CTAB micelles become saturated with peptide and the signal due to the unbound peptide predominates, resulting in a reduction of $[\theta]_{222}$. At increasing peptide

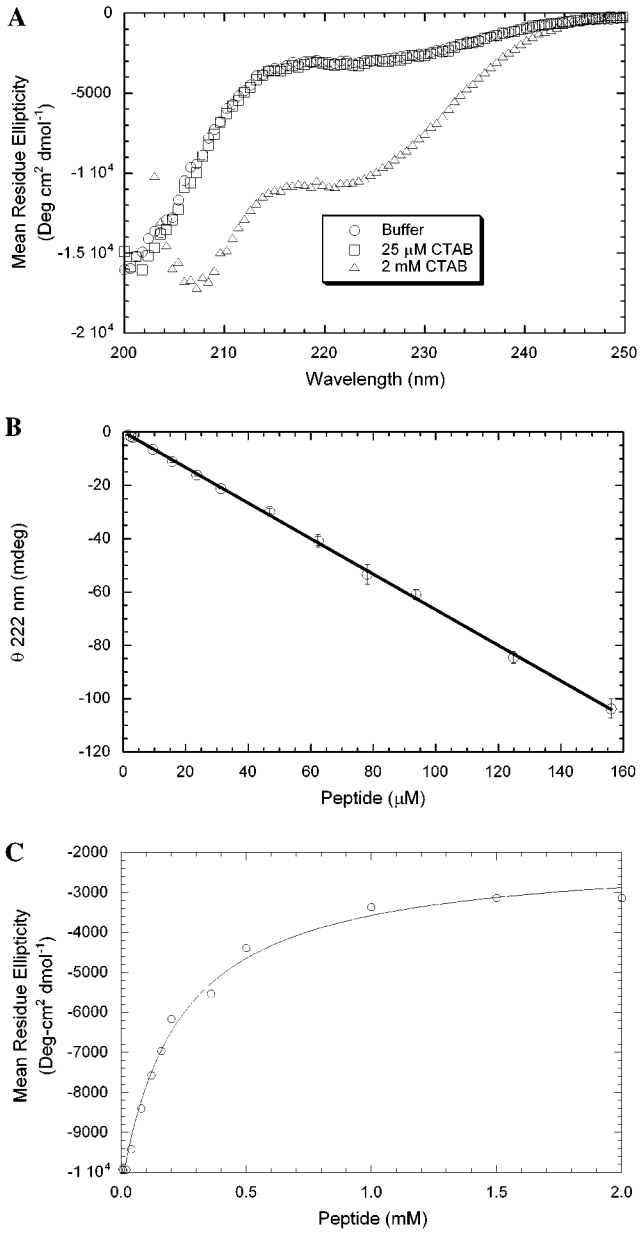

FIGURE 3: (A) CD spectra of 80 μM peptide in buffer [(○) 1 mM HEPES and 100 mM NaCl (pH 6.0)], in the same buffer in the presence of 0.025 mM CTAB (□), and in the same buffer in the presence of 2 mM CTAB (△), all at 25 °C. For ease of viewing, every fourth data point is shown. (B) Ellipticity at 222 nm of the peptide in 1 mM HEPES and 100 mM NaCl (pH 6.0) containing 0.025 mM CTAB, as a function of peptide concentration. The observed ellipticity is a linear function of peptide concentration, indicating no binding to the CTAB monomer or self-association. The mean residue ellipticity for these points was -2770 ± 104 deg cm^2 dmol^{-1} (mean ± standard deviation). (C) Mean residue ellipticity (222 nm) of the peptide at various concentrations, all in the presence of 2 mM CTAB [1 mM HEPES (pH 6.0) and 100 mM NaCl], at 25 °C. The ordinate shows ellipticity at 222 nm. Data were analyzed using the equation derived in the text. Nonlinear least-squares analysis gave a K_d of $(2.3 \pm 0.3) \times 10^{-4}$ M.

concentrations, the mean residue ellipticity approaches a value of approximately -2800 deg cm^2 dmol^{-1}, the value found for the peptide in the presence of CTAB monomers (see Figure 3B). The data in Figure 3C were analyzed as representing an equilibrium between a CTAB micelle-induced helical structure and a mostly random coil peptide found in the presence of the CTAB monomer:

$$\text{peptide} + \text{CTAB} \rightleftharpoons \text{complex}$$

$$K = \frac{[\text{peptide}][\text{CTAB}]}{[\text{complex}]}$$

where K is the equilibrium constant for the interaction. (K is not a perfectly rigorous thermodynamic parameter for two reasons. First, the ordinate axis actually represents two species: the CTAB monomer and CTAB micelles. Second, the concentration of CTAB monomer may be a function of peptide; that is, mixed micelles may form between the peptide and the detergent. In other words, multiple equilibria, of which K is an observable average, are possible.) K was calculated as before, i.e., from the relationship between the observed mean residue ellipticity and its contributing mole fractions. Nonlinear least-squares analysis of the data, shown in Figure 3C, yields a K of 2.3×10^{-4} M.

Binding of Zn^{2+} to Peptide−CTAB Complexes. To assess the ability of the CTAB-associated peptide to bind Zn^{2+}, the ellipticity of the peptide was measured in the presence of 2 mM CTAB and at various concentrations of $ZnCl_2$. In these experiments, the peptide was present at 0.1 mM, conditions under which, as the previous data show, the helical content of the peptide is close to the maximum shown in Figure 3C. Experiments indicated that the addition of Zn^{2+} to the CTAB−peptide mixture induced a small but reproducible decrease in the negative ellipticity. As shown in Figure 4A, the CD spectra remained most consistent with that of a helix, but the negative ellipticities became progressively smaller as the Zn^{2+} concentration increased.

These data were analyzed according to the following equilibrium:

$$\text{CTAB−peptide complex} + Zn^{2+} \rightleftharpoons Zn^{2+}\text{−CTAB−peptide ternary complex}$$

where Zn^{2+}−CTAB−peptide ternary complex refers to the complex described in the previous section. Accordingly, the K_d is given by the equation

$$K_d = \frac{[\text{CTAB−peptide}][Zn^{2+}]}{[\text{ternary complex}]} = \frac{([\theta]_{tcx} - [\theta]_{obs})[Zn^{2+}]}{[\theta]_{obs} - [\theta]_{complex}}$$

where $[\theta]_{complex}$ again refers to the mean residue ellipticity of the CTAB−peptide complex, but $[\theta]_{tcx}$ refers to the mean residue ellipticity of a CTAB−peptide−Zn^{2+} ternary complex. Nonlinear least-squares analysis of the data, shown in Figure 4B, yields a K_d of 2.1×10^{-4} M.

A priori, two explanations might account for the fact that Zn^{2+} lowers the mean residue ellipticity of the peptide associated with CTAB micelles. Zn^{2+} could promote a structural transition toward a state of lesser negative ellipticity. Alternatively, Zn^{2+} could promote dissociation of the peptide from the detergent micelle. That the Zn^{2+} effect is saturable suggests the former; however, to confirm that Zn^{2+} promotes a structural transition in the bound peptide, and not dissociation from the micelle, the affinity of the peptide for the detergent was measured in the presence of Zn^{2+} so that the level of binding of the peptide to CTAB would be measured under conditions in which the ternary complex would be present. The fact that strong solutions of the peptide

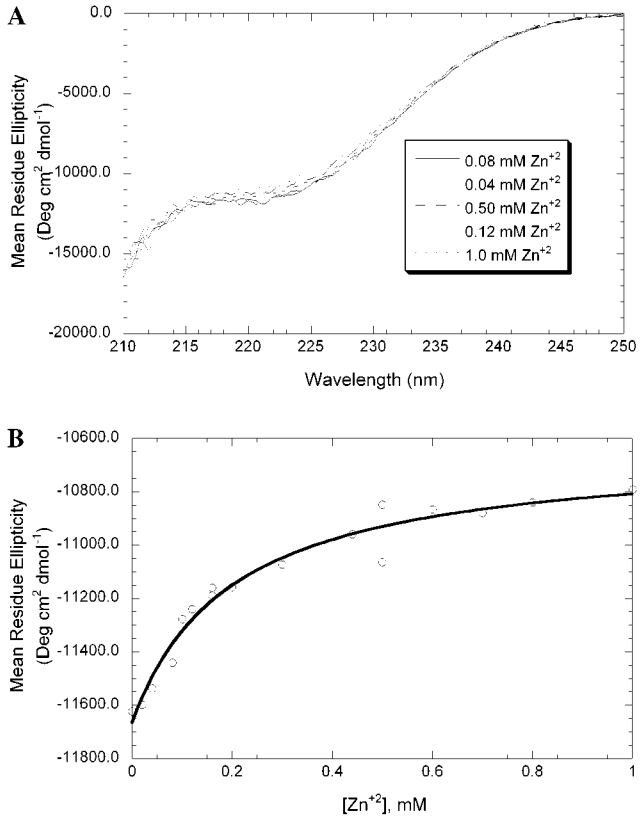

FIGURE 4: (A) CD spectra of the peptide in the presence of CTAB, at various Zn^{2+} concentrations. Conditions were chosen so that the preponderance of peptide would be associated with CTAB micelles. (B) As the Zn^{2+} concentration increases, the CD spectra remain most consistent with that of a helix, but the negative ellipticities became progressively smaller. Ellipticities at 222 nm were analyzed as described in the text. Nonlinear least-squares analysis yielded a K_d of $(2.1 \pm 0.4) \times 10^{-4}$ M.

and Zn^{2+} did not remain soluble imposed certain constraints on this experiment. Specifically, it was impossible to perform this experiment under conditions in which Zn^{2+} would saturate the peptide−CTAB complex, i.e., at Zn^{2+} concentrations of >1 mM. Consequently, this experiment was carried out at 0.1 mM Zn^{2+}, which is well below saturation. The data, shown in Figure 5, were analyzed as described above, and indicated a K of $(1.7 \pm 0.4) \times 10^{-4}$ M for the peptide's association with CTAB in the presence of Zn^{2+}. This value is smaller than the measured value in the absence of Zn^{2+} [$K = (2.3 \pm 0.3) \times 10^{-4}$ M], but within the error in the curve fitting routine, the two values are not distinguishable. Nevertheless, it seems clear that Zn^{2+} does not decrease the affinity of the peptide for CTAB, and therefore, the above data are most consistent with a Zn^{2+}-induced structural change in the peptide−CTAB complex.

Peptide Surface Isotherms in the Presence and Absence of Zn^{2+}. The peptide was designed to be amphiphilic in the π-helical, but not in the α-helical, conformation. To assess directly whether the peptide was amphiphilic, the surface isotherms of the peptide at the air−water interface were measured using subphases with and without Zn^{2+}. As shown in Figure 6A, the peptide formed moderately stable monolayers when spread over a subphase of buffer without Zn^{2+}, as shown by a monolayer collapse pressure of approximately 10.8 mN/M. Figure 6B shows the effect of adding Zn^{2+} to the subphase. The addition of Zn^{2+} increased the collapse

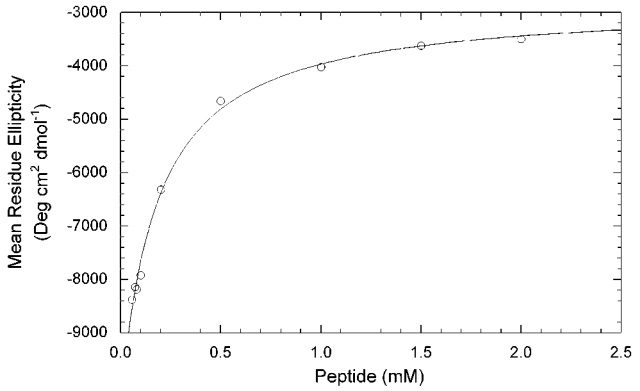

FIGURE 5: Binding of peptide to CTAB in the presence of 0.1 mM $ZnCl_2$. Nonlinear least-squares analysis of the data indicates a K of $(1.7 \pm 0.4) \times 10^{-4}$ M. Although suggesting an increase in the peptide's affinity for CTAB in the presence of Zn^{2+} compared to its affinity in the absence, the equilibrium constants are not distinguishable within experimental error. Nevertheless, this result confirms that the binding of Zn^{2+} to the peptide−CTAB complex induces a structural change associated with a loss of ellipticity, and not dissociation of peptide, which would have been associated with a decline in the peptide's affinity for CTAB.

Table 1: Summary of Parameters Obtained from Analysis of Surface Pressure−Area Isotherms

	0 mM subphase Zn^{2+}	10 mM subphase Zn^{2+}
collapse pressure (mN/M)	10.8	18.8
A_0 (excluded area, Å^2/amino acid)	28.3	22.5
κ (compressibility, M/mN)	0.029	0.019

pressure to approximately 14 mN/m at 1 mM Zn^{2+} (not shown) and to approximately 18.8 mN/M at 10 mM Zn^{2+}. For surface pressures of <1 mN/m, the isotherms were analyzed using the equation of a two-dimensional gas

$$\pi(A - nA_0) = nRT$$

in which π is the surface pressure (millinewtons per meter), A is the area (square centimeters), n is the number of moles of the peptide at the interface, A_0 is the molar exclusion area, R is the gas constant, and T is the absolute temperature. When π is greater than 1 mN/m, surface isotherms usually deviate from the above equation, as was observed for this peptide. Accordingly, when π was greater than 1 mN/M, data were analyzed according to the equation (*22*)

$$\pi[A - nA_{00}(1 - \kappa\pi)] = nkT$$

where A_{00} is the molar exclusion area of the peptide at the surface, extrapolated to $\pi = 0$. The term κ has the units of compressibility, and k is a constant with the same units as the gas constant. As shown in Figure 6A, the isotherm fit this equation for values of π between 1 mN/M and the monolayer collapse pressure. The peptide became more compact at the interface in the presence of Zn^{2+}, as shown by the reduction of the excluded area from 28.3 to 22.5 Å^2 per amino acid. Whereas random coil peptides typically have areas of approximately 50 Å^2 per amino acid, a value of 22.5 Å^2 per amino acid is compatible with the existence of secondary structure at the interface (*23*). These values, summarized in Table 1, suggest that the peptide adopts a secondary structure at the surface, and that the addition of

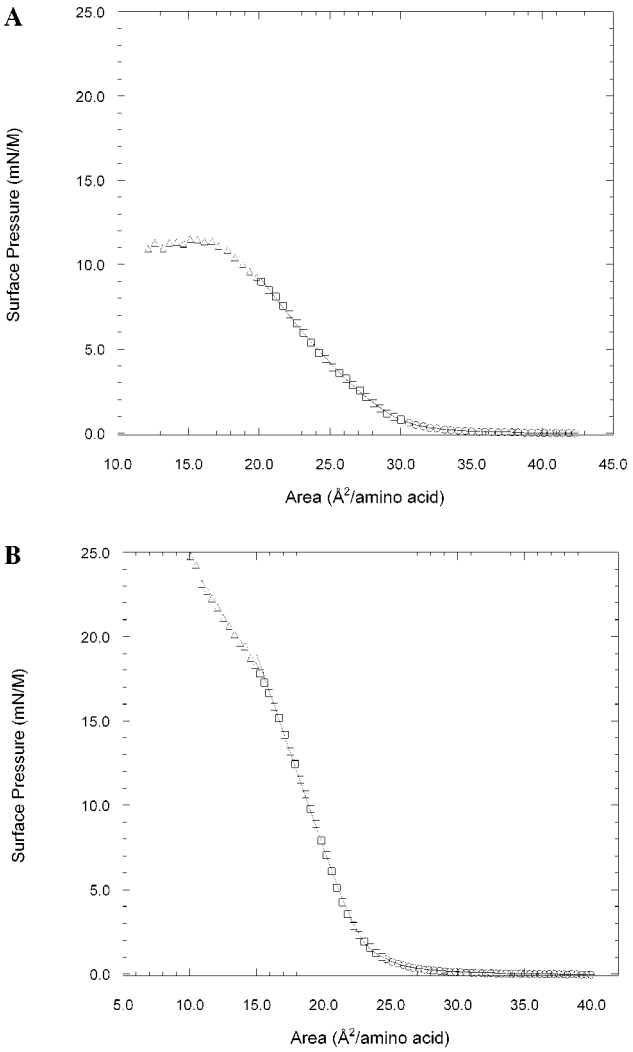

FIGURE 6: Surface isotherms of peptide spread over a subphase of 1 mM HEPES and 100 mM NaCl (pH 6.0) (A), and also containing 10 mM $ZnCl_2$ (B). For both curves, fitting was as described in the text, and symbols are as follows: (○) $\pi < 1$ mN/M, (□) $\pi > 1$ mN/M and below the collapse pressure, and (△) collapsed monolayer.

Zn^{2+} alters that conformation, rendering it more amphiphilic in the process. Most importantly, since the Zn^{2+} binding histidine residues occur with i, $i + 5$ spacing, these data are consistent with stabilization of a π-helical conformation in the amphiphilic environment of the air−water interface.

Thermal Stability. The thermal stabilities of the peptide species in 50% TFE were assessed by comparing the thermal denaturation profiles of the peptide in 50% TFE, and in 50% TFE containing 1 mM $ZnCl_2$. The ellipticity of the peptide declined as the temperature increased (Figure 7A). In 50% TFE, the transition was not a sharp one, although the addition of Zn^{2+} made the transition somewhat sharper. As a first approximation, van't Hoff analyses were carried out by modeling the transition as an equilibrium between a low-temperature (L) (i.e., helical) and high-temperature (i.e., coil) state (H) of the peptide:

$$L \rightleftharpoons H$$

The fraction of the low- and high-temperature species can

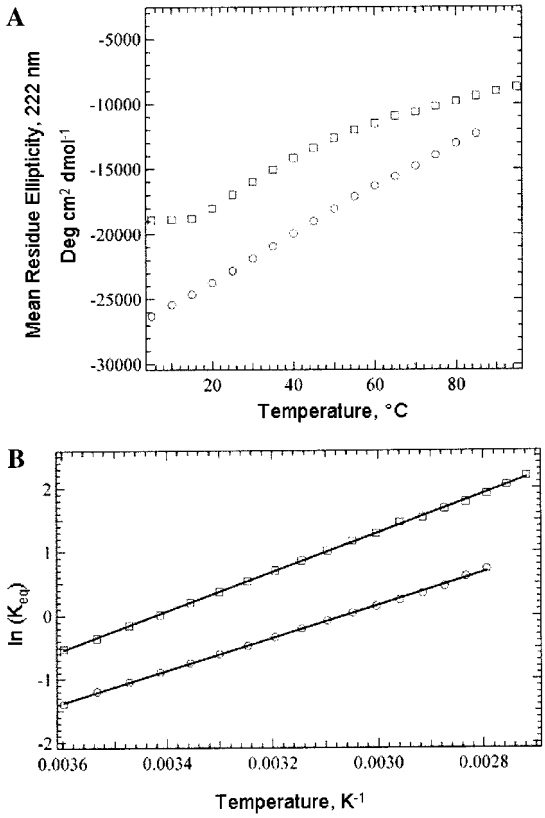

FIGURE 7: (A) Thermal denaturation profiles of the peptide in 50% TFE [pH 6.0 (○)] and in 50% TFE containing 1 mM $ZnCl_2$ (□). (B) van't Hoff plots for denaturation of the peptide under the conditions described for panel A. For denaturation in the presence of buffer alone (○), $\Delta H = 5.22$ kcal/mol and $\Delta S = 15.2$ cal K^{-1} mol^{-1}. For denaturation in the presence of 1 mM $ZnCl_2$ (□), $\Delta H = 6.08$ kcal/mol and $\Delta S = 20.1$ cal K^{-1} mol^{-1}.

be expressed as follows:

$$f_L + f_H = 1$$

$$f_H = \frac{\theta_{obs} - \theta_H}{\theta_L - \theta_H}$$

$$f_L = 1 - f_H = \frac{\theta_L - \theta_{obs}}{\theta_L - \theta_H}$$

where θ_{obs} is the experimentally measured ellipticity. The equilibrium constant, written in terms of the unfolding process, is

$$K_{eq} = \frac{f_H}{f_L} = \frac{\theta_{obs} - \theta_H}{\theta_L - \theta_{obs}}$$

from which van't Hoff plots (Figure 7B) were made according to the equation

$$\Delta G = -RT \ln K_{eq} = \Delta H - T\Delta S$$

$$\ln\left(\frac{\theta_{obs} - \theta_H}{\theta_L - \theta_{obs}}\right) = -\frac{\Delta H}{RT} + \frac{\Delta S}{R}$$

Heating of the peptide in 50% TFE, in the presence or absence of Zn^{2+}, induced a helix to coil transition. In the absence of Zn^{2+}, thermal unfolding of the peptide is associated with a ΔH of 5.2 kcal/mol and a ΔS of 15.9 cal

Table 2: Summary of Thermodynamic Parameters

	peptide in 50% TFE	peptide in 50% TFE and 1 mM Zn^{2+}
ΔH (kcal/mol)	5.22	6.08
ΔS (cal mol^{-1} K^{-1})	15.9	20.8
$\Delta G_{20°C}$ (kcal/mol)	0.55	−0.01
$\Delta G_{25°C}$ (kcal/mol)	0.48	−0.12

K^{-1} mol^{-1}. Adding Zn^{2+} results in an increase in both of these parameters: $\Delta H = 6.1$ kcal/mol and $\Delta S = 20.8$ cal K^{-1} mol^{-1}. This increase is especially notable in ΔS, consistent with the idea that Zn^{2+} decreases the entropy of the folded state by stabilizing a structure of the peptide. The thermodynamic parameters are summarized in Table 2.

DISCUSSION

One of the remarkable features that emerges from the past 50 years of structural biology is that amino acid polymers exist in a narrow range of secondary structures. As our analytical techniques improve, however, and as the number of solved protein and peptide structures increases, we are likely to see other structures emerge. As noncanonical structures appear, questions about their stability will naturally arise. This paper addresses the occurrence and stability of π-helical structure in an amphiphilic, metal-binding polypeptide.

The peptide described herein was designed to be a π-helical amphiphile and to bind Zn^{2+} in a π-helical fashion. Consistent with that design, the peptide formed relatively stable monolayers at the air−water interface, and underwent a random coil to helix transition when interacting with the detergent CTAB. Zn^{2+} binding was used as a probe of the *i*, *i* + 5 di-histidine metal binding motif, and indeed, the peptide was found to bind Zn^{2+} in three independent experiments. First, in 50% TFE, an α-helix-promoting solvent, it was found to undergo a Zn^{2+} binding event that reduced its mean residue ellipticity. Second, the peptide−CTAB complex was found to undergo a similar Zn^{2+} binding event that also reduced its mean residue ellipticity, although the magnitude of the effect was smaller in this case. Finally, the peptide's surface activity was modulated by the presence of Zn^{2+} in the subphase. Specifically, Zn^{2+} promoted the formation of a more stable monolayer, reduced the mean area occupied by the constituent amino acids, and reduced the compressibility of the monolayer. The effect of Zn^{2+} was therefore both to alter its structure and to render it a better amphiphile.

Because limited experimental data about the π-helix have accumulated, relating the findings described above to π-helical structure is a challenge. However, it is possible to be guided by theoretical considerations, especially where the CD measurements are concerned. In CD spectra of polypeptides, the observed signal derives from the sum of the transitions of the peptide bonds in the molecule (*24*). Therefore, it is the regularity of a conformation that leads to a strong CD signal associated with that conformation. The disruption of regularity or, equivalently, the introduction of distortion into an otherwise regular polypeptide structure would result in a reduction in the intensity of the CD signal. In a "canonical" α-helix, the backbone atoms of each residue are separated from adjacent residues by a rotation of 100° about the helical axis, and a translation of approximately 1.5 Å along it (*1*). Therefore, in a canonical *i*, *i* + 4 α-helical metal ion binding motif, the two ligating residues would be separated by 400° (i.e., 40°) of rotation and by approximately 6 Å of translation along the helical axis. If a metal ion binding motif consisting of *i*, *i* + 5 residues were to preserve typical α-helical geometry, the backbone atoms of the ligating residues would be separated from each other by 500° (i.e., 140°) of rotation and by a translation of 7.5 Å. While it would be possible for residues with sufficiently long side chains to accommodate this longer distance, they would project from nearly opposite faces of the helix, making it unlikely that they could bind a metal. Therefore, an *i*, *i* + 5 metal binding motif cannot preserve α-helical backbone geometry. Thus, an *i*, *i* + 5 structure must be distorted, and by the reasoning above, for the CD observation associated with that distortion there must be a reduction in the intensity of the helical signature. An *i*, *i* + 5 interaction is equally unlikely to be accommodated by the other common peptide secondary structures. For example, in 3_{10}-helices, *i*, *i* + 5 residues would be separated by a potentially manageable 600° (i.e., 120°) of rotation, but by an unmanageable translation of 10 Å (*25*). Canonical γ-turns involve three amino acids making an *i*, *i* + 2 hydrogen bond, and β-turns (types I−VIII) employ four residues making *i*, *i* + 3 hydrogen bonds (*25*), and position *i*, *i* + 5 side chains on opposite faces of the structure. Thus, none of these structures are capable of accommodating an *i*, *i* + 5 metal binding motif.

Geometric reasoning like that described above helps to explain the decline in the negative ellipticity when this peptide binds Zn^{2+} as the introduction of distortion. However, additional information about the structure is available through comparison of the manner in which the Zn^{2+} binding occurs in 50% TFE and in the peptide−CTAB complex. In 50% TFE, the mean residue ellipticity of the peptide at 222 nm was −23000 deg cm^2 $dmol^{-1}$. The addition of Zn^{2+} caused a large, progressive, and saturable decrease in the negative ellipticity, to a limiting value of −15400 deg cm^2 $dmol^{-1}$. As described above, this decrease in ellipticity is consistent with the induction of a π-helical turn in the center of the peptide, i.e., in the vicinity of the two His residues. In the case of Zn^{2+} binding by the peptide−CTAB complex, the transition is from a state whose limiting mean residue elipticity at 222 nm is −11600 deg cm^2 $dmol^{-1}$ to one whose limiting ellipticity is −10600 deg cm^2 $dmol^{-1}$. Compared to the situation in 50% TFE, this is a smaller percentage change on Zn^{2+} binding, indicating that the structural change is less pronounced. When the observation that the peptide−CTAB complex has a greater Zn^{2+} affinity than the peptide alone in 50% TFE is considered, this suggests that the CTAB-bound peptide must be in a conformation predisposed to binding Zn^{2+}. Because the peptide is not predicted to be an amphiphilic α-helix, but rather a continuous amphiphilic π-helix, acquisition of π-helical structure should render the peptide more amphiphilic. Zn^{2+} binding increases the monolayer collapse pressure, decreases its surface area per amino acid, and decreases its compressibility of the monolayer, all observations demonstrating greater amphiphilicity and greater ordering at the interface in the Zn^{2+}-bound state. Thus, our data suggest that the peptide described in this paper behaves as a π-helical amphiphile in the presence of CTAB and $ZnCl_2$.

Table 3: Dihedral Angles for the π-Helix in Soybean Lipoxygenase[a]

residue	ϕ (deg)	ψ (deg)	residue	ϕ (deg)	ψ (deg)
Tyr493	−65	−38	Trp500[b]	−67	−56
His494[b]	−64	−50	Leu501[b]	−70	−61
Gln495[b]	−67	−48	Asn502[b]	−65	−19
Leu496[b]	−83	−48	Thr503[b]	−117	−65
Met497[b]	−92	−59	His 04[b]	−60	−59
Ser498	−63	−37	Ala505	−69	−41
His499[b]	−100	−59	Ala506	−66	−31

[a] The data in this table were obtained using the dihedral angle measure function in the Insight II software package (Biosym), using the coordinates for soybean lipoxygenase (PDB entry 2SBL) that were available in the Protein Data Bank (*32*). [b] These residues are those in which either ϕ, ψ, or both fall outside of the expected range of dihedral angles for α-helices.

This conclusion then raises the question of the nature of a π-helix. Has the peptide described in this paper adopted the structure Low and Baybutt proposed in 1952 (*3*)? At this point, it is not possible to answer this question precisely. However, some insight into the possibility of that structure can be gained from the descriptions of existing π-helices. Backbone distortions are common features of these π-helices. In soybean lipoxygenase (*26*), residues 493−506 form a π-helix, but unlike the α-helical segments around it, the π-helix has irregular dihedral angles. In the original proposal (*3*), the π-helix was defined as having ϕ and ψ angles of −57° and −70°, respectively. Ramachandran predicted that the π-helix would be marginally stable because these dihedral angles place amino acids in the "extreme limit" region of conformational space, meaning that atoms are found as close together as they had ever been found in the crystal structures from the period (*4*). In fact, none of the amino acids in the π-helix in soybean lipoxygenase have these dihedral angles (Table 3), and the mean values of ϕ and ψ in this π-helix are −74.86° and −47.93°, respectively. The dihedral angles in the lipoxygenase π-helix are also outside, and sometimes far from (*26*), the range expected for α-helices [$\phi = -55°$ to −70°, and $\psi = -30°$ to −45° (*27*)]. Among the 14 residues in the structure, there are only four which do have α-helical dihedral angles (Tyr493, Ser498, Ala505, and Ala506), and only the serine is in the center of the helix. The other three of these residues are at the ends of the π-helix, i.e., are also involved in α-helical interactions with the adjacent α-helices.

Such distortions are not confined to lipoxygenase. In fact, deviation of dihedral angles from their canonical values appears to be a common feature of the π-helices which have been observed. They occur, for example, in the π-helical turn in fumarase C from *Escherichia coli* (*7*) in which the helical backbone is distorted around Asn B135, in a manner reminiscent of that found at Thr502 and His499 in lipoxygenase (*26*). The same pattern is seen at amino acid 311 in catalase from *Penicillium vitale* (*6*) in π-helix E at Cys157 and at Asp186 in cytochrome P450 (*8*). Evidence for these types of distortions has also been presented in molecular dynamic simulations (*11*−*13*). This common arrangement may be functional in that it positions the amido hydrogen atom of the affected residue such that it can recover some of the van der Waals contacts lost in the expansion of the helix. Thus, it may be that the amino acids involved in π-helices do not have "π-helical" dihedral angles because those angles are impossible to sustain over a number of residues, and because distorting those dihedral angles may actually confer stability.

Thus, in contrast to α-helices, π-helices are unlikely to have dihedral angles of inherently low conformational energy, and those π-helices that exist are probably stabilized through other forces, such as tertiary contacts, metal ion binding, or amphiphilicity. The peptide described in this paper is stabilized by the latter two factors. The affinity of the peptide for Zn^{2+} when bound to CTAB, and thus in a conformation approximating a π-helical turn, was equal to 2.1×10^{-4} M (K_d). A comparison of this value with that of similar Zn^{2+} binding peptides with His residues in *i*, *i* + 4 spacing should reflect the energetic costs of forming a π-helical turn. Ghadhiri and Choi (*28*) describe a 17-amino acid α-helical peptide containing two His residues with *i*, *i* + 4 spacing. The peptide had an affinity for Zn^{2+} of 75 μM at pH 8, and an affinity for Cu^{2+} of 66 μM at pH 5. These values appear to be typical; in a recent review, Regan (*29*) noted that the affinity of a protein or peptide containing two ligands for a divalent metal ion is generally in the range from 2×10^{-4} to 2×10^{-6} M. The Zn^{2+} affinity of the peptide described in this paper is on the edge of this range, and ∼1 order of magnitude above the mean value. Thus, to a first approximation, the energy difference between an *i*, *i* + 4 Zn^{2+}-binding motif ($K_d = 2 \times 10^{-5}$ M, $\Delta G = 6.4$ kcal/mol) and the *i*, *i* + 5 Zn^{2+} binding peptide described in this paper ($K_d = 2.1 \times 10^{-4}$ M, $\Delta G = 5.1$ kcal/mol) is on the order of 1 kcal/mol. Although it does not appear that the introduction of a π-helical distortion into an α-helical structure has been previously investigated, Craik (*30*) has studied the Zn^{2+}-induced introduction of distortion in a serine protease. The protein was modified so that one of the histidines in the catalytic triad could form a di-histidine metal binding motif if it rotated 90° out of its native position. This work, which observed an inhibition constant of 128 μM for Zn^{2+}, also suggests that ordinary Zn^{2+} affinities are lowered by approximately 1 order of magnitude when coupled with the distortion of an otherwise native structure.

More direct analysis of the change in stability induced by *i*, *i* + 5 interactions comes from thermal denaturation. As shown in Table 2, the addition of Zn^{2+} results in a moderate increase in ΔH. There is a more marked increase in ΔS resulting from the addition of Zn^{2+}, consistent with the notion that Zn^{2+} binding decreases the entropy of the folded state of the peptide. This "entropic penalty" probably derives in part from the organization of the histidine side chains which occurs upon Zn^{2+} coordination, and would be expected for any such restriction of side chain motion. Yet, in this case the peptide has an additional, local π-helical character; the formation of an *i*, *i* + 5 metal binding site organizes six amino acid residues, rather than the five which are organized in an α-helical metal binding site. Rohl and Doig have addressed the issue of entropy in π-helix formation theoretically. They conclude that it is sufficiently destabilizing that spontaneous π-helix formation cannot be expected (*31*). Our data underscore the importance of entropy in π-helical situations and, more generally, the importance of compensatory external stabilization.

Overall indications of the change in peptide stability due to Zn^{2+} binding can be gleaned from the values for ΔG at 25 °C (Table 2). Whereas ΔG for the peptide in 50% TFE

is 0.48 kcal/mol (i.e., more of the peptide is in the folded state than in the unfolded state), ΔG after the addition of Zn^{2+} is −0.12 kcal/mol. Thus, the effect of Zn^{2+} on the stability of the current peptide contrasts with that in α-helical situations (*28*), in which binding of Zn^{2+} clearly enhances the peptide's stability, and our data indicate that the basis for the change in stability is significantly entropic in nature.

π-Helices are relatively unstable, but they are not so unstable that they cannot be constrained to form, and hence are found in proteins; in this work, we have investigated a short π-helix peptide. The relative instability of the π-helix may account for its rarity and the necessity of constraining it to form. But what accounts for its occurrence? π-Helices could confer a number of potentially useful properties upon the proteins in which they occur. Because of their reduced stability, they could relax to an α-helical state or could be capable of switching between α- and π-helical states attendant upon association with ligands or metal ions. Weaver (*15*) has suggested that π-helices are evolutionary responses to specific demands at protein binding sites, and that they lead to functional and unique structural interactions. As suggested above, π-helices can modulate amphiphilicity, and hence, one such functional interaction may occur in the region of apolipoprotein E (amino acids 41−61), to which the peptide discussed in this paper is distantly related. ApoE must function in a lipid-associated state and also in a lipid-free state. The crystal structure of the N-terminal thrombolytic domain in its delipidated form shows this region to consist of a short α-helix separated by turns from two long α-helices in a four-helix bundle (*19*). The structure in the lipid-bound form is unknown, but has been shown to undergo reorientation as the protein moves between the lipidated and delipidated states (*32*), and amino acids 41−61 have been proposed to be important in that process (*20*). The peptide described in this paper switches between conformational states, and a marginally stable π-helical conformation may facilitate such switching in a context like that of ApoE.

REFERENCES

1. Pauling, L., and Corey, R. B. (1951) *Proc. Natl. Acad. Sci. U.S.A. 37*, 235−240.
2. Pauling, L., and Corey, R. B. (1951) *Proc. Natl. Acad. Sci. U.S.A. 37*, 241−250.
3. Low, B. W., and Baybutt, R. B. (1952) *J. Am. Chem. Soc. 74*, 5806−5807.
4. Ramachandran, G., and Sasisekharan, H. (1968) *Adv. Protein Chem. 23*, 284−438.
5. Donohue, J. (1953) *Proc. Natl. Acad. Sci. U.S.A. 39*, 470−478.
6. Vainshtein, B. K., Melik-Adamyan, W. R., Barynin, V. V., Vagin, A. A., Grebenko, A. I., Borisov, V. V., Bartels, K. S., Fita, I., and Rossman, M. G. (1986) *J. Mol. Biol. 188*, 49−61.
7. Weaver, T., and Banaszak, L. (1996) *Biochemistry 35*, 13955−13965.
8. Hasemann, C. A., Kurumbail, R. G., Sekhar, S. B., Peterson, J. A., and Deisenhofer, J. (1995) *Structure 2*, 41−62.
9. Boyington, J. C., Gaffney, B. J., and Amzel, L. M. (1993) *Science 260*, 1482−1486.
10. Boyington, J. C., Gaffney, B. J., Amzel, L. M., Doctor, K. S., and Mavrophilipos, D. V. (1995) *Ann. N.Y. Acad. Sci. 744*, 310−313.
11. Duneau, J.-P., Genest, D., and Genest, M. (1996) *J. Biomol. Struct. Dyn. 13*, 753−769.
12. Duneau, J.-P., Crouzy, S., Chapron, Y., and Genest, M. (1999) *Biophys. Chem. 76*, 35−53.
13. Lee, K.-H., Benson, D. R., and Kuczera, K. (2000) *Biochemistry 39*, 13737−13747.
14. Rajashankar, K. R., and Ramakumar, S. (1996) *Protein Sci. 5*, 932−946.
15. Weaver, T. (2000) *Protein Sci. 9*, 201−206.
16. Kaiser, E. T., and Kézdy, F. J. (1983) *Proc. Natl. Acad. Sci. U.S.A. 80*, 1137−1143.
17. Chattopadhyay, A., and London, E. (1984) *Anal. Biochem. 139*, 408−418.
18. Braddock, D. T., Mercurius, K. O., Subramanian, R. M., Dominguez, S. R., Davies, P. F., and Meredith, S. C. (1996) *Biochemistry 35*, 13975−13984.
19. Wilson, C., Wardell, M. R., Weisgraber, K. H., Mahley, R. W., and Agard, D. A. (1991) *Science 252*, 1817−1822.
20. Luo, P., Braddock, D. T., Subramanian, R. M., Meredith, S. C., and Lynn, D. G. (1994) *Biochemistry 33*, 12367−12377.
21. Martell, A. E., and Smith, R. M. (1975) *Critical Stability Constants*, Vols. 2 and 3, Plenum Press, New York.
22. Retzinger, G. S., Meredith, S. C., Takayama, K., Hunter, R. L., and Kézdy, F. J. (1981) *J. Biol. Chem. 256*, 8208−8216.
23. Lau, S. H., Rivier, J., Vale, W., Kaiser, E. T., and Kezdy, F. J. (1983) *Proc. Natl. Acad. Sci. U.S.A. 80*, 7070−7074.
24. Cantor, C. R., and Schimmel, P. R. (1971) *Biophysical Chemistry: Techniques for the Study of Biological Structure and Function*, Vol. 2, W. H. Freeman and Co., New York.
25. Creighton, T. E. (1993) *Proteins: Structures and Molecular Properties*, W. H. Freeman and Co., New York.
26. Gaffney, B. J. (1996) *Annu. Rev. Biophys. Biomol. Struct. 25*, 431−459.
27. Barlow, D. J., and Thornton, J. M. (1988) *J. Mol. Biol. 201*, 601−609.
28. Ghadiri, M. R., and Choi, C. (1990) *J. Am. Chem. Soc. 112*, 1630−1632.
29. Regan, L. (1993) *Annu. Rev. Biophys. Biomol. Struct. 22*, 257−287.
30. Higaki, J. N., Haymore, B. L., Chen, S., Fletterick, R. J., and Craik, C. S. (1990) *Biochemistry 29*, 8583−8586.
31. Rohl, C. A., and Doig, A. J. (1996) *Protein Sci. 5*, 1687−1696.
32. Lu, B., Morrow, J. A., and Weisgraber, K. H. (2000) *J. Biol. Chem. 275*, 20775−20781.
33. Berman, H. M., Westbrook, J., Feng, Z., Gilliland, G., Bhat, T. N., Weissig, H., Shindyalov, I. N., and Bourne, P. E. (2000) *Nucleic Acids Res. 28*, 235−242.

BI0155605